Optical and structural properties of Mn-doped magnesium titanates fabricated with excess MgO

L. Borkovska, L. Khomenkova, T. Stara, I. Vorona, V. Nosenko, O. Gudymenko, V. Kladko, K. Kozoriz, C. Labbé, Julien Cardin, et al.

Optical and structural properties of Mn-doped magnesium titanates fabricated with excess MgO

L. Borkovska [a,*], L. Khomenkova [a], T. Stara [a], I. Vorona [a], V. Nosenko [a], O. Gudymenko [a], V. Kladko [a], K. Kozoriz [a], C. Labbé [b], J. Cardin [b], J.-L. Doualan [b], T. Kryshtab [c]

[a] V. Lashkaryov Institute of Semiconductor Physics of the NAS of Ukraine, 45 Prospect Nauky, 03028, Kyiv, Ukraine
[b] CIMAP, 6 Blvd Maréchal Juin, Caen, France
[c] Instituto Politécnico Nacional – ESFM, Av. IPN, Ed.9 U.P.A.L.M., 07738, Mexico D.F., Mexico

Keywords:
Oxide materials
Ceramics
Point defects
Luminescence
Electron paramagnetic resonance
X-ray diffraction

A B S T R A C T

Optical and structural properties of ceramics based on Mn-doped magnesium titanates synthesized by sintering in air at 1200 °C of MgO and TiO_2 powders of different molar ratios ranging from $MgTiO_3$ to Mg_2TiO_4 stoichiometric compositions were studied. The influence of excess MgO on Mn incorporation in crystal lattice of $MgTiO_3$ was also investigated. The Mn^{4+} ions substituted Ti^{4+} sites were controlled by the photoluminescence (PL) and diffuse reflectance spectroscopy, and the Mn^{2+} ions on Mg^{2+} sites were monitored by electron paramagnetic resonance (EPR). The ceramics produced using equimolar ratio of MgO and TiO_2 composed of a major $MgTiO_3$ and a minor $MgTi_2O_5$ crystal phases, and those made with excess MgO contained $MgTiO_3$ and Mg_2TiO_4 phases in different proportions. The EPR study showed that Mn incorporated in $MgTiO_3$ synthesized under 1:1 M ratio as Mn^{2+} ion mainly. This agreed with low intensity of Mn^{4+} red PL ascribed to low concentration of Mn^{4+} centers and partial absorption of the UV excitation light by the $MgTi_2O_5$ phase. The Mn-doped $MgTiO_3$ synthesized with excess MgO of 19 and 50 mol.% showed increased Mn^{4+} red PL by a factor 30–50, enhanced Mn^{4+} optical absorption and more than ten times decreased Mn^{2+} EPR signal. The Mg_2TiO_4 phase was found to be under compressive strains attributed to the presence of Mg vacancies and demonstrated Mn^{4+} red PL with modified spectrum shape and decay behavior. It is concluded that in $MgTiO_3$ the excess MgO facilitates the incorporation of Mn onto Ti^{4+} site and can be used for the increasing of Mn^{4+} PL intensity.

1. Introduction

For decades the interest to magnesium metatitanate, $MgTiO_3$, was motivated by its application in low loss microwave dielectric resonators as a material with high dielectric constant (ε_r~17) and high-quality factor (Q_f~160,000 GHz) [1,2]. To improve the performance of $MgTiO_3$-based microwave dielectric ceramics the effect of doping with metal ions like Ni, Zn, Co, Mn and others on microstructure and dielectric properties of $MgTiO_3$ has been studied [3–5]. In particular, the doping with Mn^{4+} and W^{6+} was shown to be efficient in producing $MgTiO_3$ ceramics of high insulation resistance when sintering is carried out in reducing atmosphere [6]. It was found that the effect of dopants on intrinsic dielectric losses of $MgTiO_3$ ceramics depended on whether they form a distinct second phase or a solid solution with $MgTiO_3$, and in the last case, intrinsic losses were strongly affected [3].

Recently, $MgTiO_3$ has attracted attention as a suitable matrix for Mn^{4+} ions [7–10]. Mn^{4+} activated titanates are known as the promising red phosphors for application in phosphor converted light emitting diodes, LEDs, which use blue LED chip for excitation [11]. In fact, titanate compounds are known for their excellent thermal stability and environmental safety, as well as the substitution of Mn^{4+} for Ti^{4+} in octahedral coordination is highly feasible due to the similar ionic radius and the same oxidation state [11]. The Mn^{4+} ion substituted Ti^{4+} cation in crystal lattice of $MgTiO_3$ shows deep red photoluminescence (PL) at about 701 nm under UV and blue-green excitation [7,10,12]. In the compounds of $ATiO_3$ (A = Sr, Ba, Ca, Mg), the energy of the emitting $^2E \rightarrow {}^4A_2$ transition is the largest in $MgTiO_3$ due to the smallest fraction of covalence in the Mn^{4+}-O^{2-} bonding [7]. Because of the thermal quenching of Mn^{4+} PL at room temperature the $MgTiO_3$:Mn^{4+} red phosphor does not seem to be attractive for the use in lighting. At the same time, the temperature dependent characteristics of Mn^{4+} red emission in $MgTiO_3$ enable the application of this phosphor in

luminescence temperature probes [8].

The Mn-doped $MgTiO_3$ can be easy synthesized via sintering in the air of equimolar mixture of MgO and TiO_2 powders [4,6,13]. However, high temperatures (1000−1300 °C) required for sintering of $MgTiO_3$ result in low intensity of Mn^{4+} PL [14]. This last result promoted the development of alternative approaches for low temperature synthesis of Mn^{4+} activated $MgTiO_3$ such as firing in the air of a magnesium-titanium complex tartrate [14] or the combination of sol-gel method with annealing in the melt of salts [7].

To enhance Mn^{4+} luminescence, it is necessary to increase the number of Mn^{4+} centers in a matrix, preventing energy migration between the ions, and to decrease concentration of Mn dopants in another charge states such as Mn^{3+} and Mn^{2+}. Above mentioned states are supposed to behave as the competitive centers of radiative [15] or nonradiative recombination [16,17]. In particular, the adding a small amount of Mg in the form of MgO [18,19], $MgCO_3$ [20] or MgF_2 [21] to raw oxide mixture was found to be a feasible way to increase the intensity of Mn^{4+} red luminescence in oxide matrixes. Several mechanisms were proposed for explanation of the effect. In Mn^{4+} activated $CaAl_{12}O_{19}$, the synergetic effect of flux and charge compensation by MgF_2 resulted in the increment of the fraction of ions in the +4 state was assumed [21]. Alternatively, in Mn^{4+} activated $CaAl_{12}O_{19}$ [22] and $Y_3Al_5O_{12}$ [20], the Mg^{2+} dopants were supposed to suppress adverse energy migration among neighboring Mn^{4+} activators and/or to behave as charge compensating ions, which reduce concentration of O^{2-} quenching centers. Recently [23], the Mn^{4+}-doped Mg_2TiO_4 phosphors fabricated with an excess MgO showed the increased Mn^{4+} red PL and the decreased Mn^{2+} electron paramagnetic resonance (EPR) signal. It has been concluded that an excess MgO stimulates substitution of manganese for Ti site in +4 charge state.

The effect of Mg-doping on crystal phase formation and dielectric characteristics of $MgTiO_3$ ceramics was also investigated [5,24]. In particular, a dramatic enhancement of Q_f value up to 262,900 GHz was demonstrated in 3 wt% MgF_2-doped $MgTiO_3$ ceramic sintered at 1300 °C [5]. This effect was explained by the influence of MgF_2 on crystal phase formation (the Mg-rich compound inhibited the formation of $MgTi_2O_5$ and promoted the formation of Mg_2TiO_4), the production of the liquid phase, which optimizes the pore structure of ceramics and improves the sintering process, as well as the decrease of the leakage current owing to the grain boundary barrier effect. Similarly, the $MgTiO_3$ ceramics obtained by sintering at 1300 °C of MgO nanopowders and TiO_2 nanowires with excess MgO (in 1.23:1 M ratio) demonstrated strongly enhanced quality factor Q_f ~300,000 GHz explained by more uniformly distributed grain size and dense compact [24].

The adding of excess MgO over those necessary to obtain stoichiometric composition of $MgTiO_3$ is known to result in formation of Mg_2TiO_4 crystal phase side-by-side with the $MgTiO_3$ [10,25]. It has been shown [10] that Mn-doped magnesitum titanate phosphors synthesized under different MgO to TiO_2 molar ratio in the range from 1:1 to 2:1 shows two PL bands caused by radiative transitions of Mn^{4+} ions substituted Ti^{4+} site ions in the $MgTiO_3$ and Mg_2TiO_4, and relative intensity of each band depends on the content of corresponding crystal phase. However, the influence of excess MgO on Mn charge state in the $MgTiO_3$ was not investigated.

In this work, the effect of excess MgO on formation of crystal phases and the peculiarities of manganese incorporation (specifically its charge state) into crystal lattice of $MgTiO_3$ synthesized by conventional solid state reaction was investigated. We show that Mn charge state in the $MgTiO_3$ as well as Mn^{4+} emission spectra in the Mg_2TiO_4 critically depend on the ratio of Mg_2TiO_4 an $MgTiO_3$ phases in the final product. We hope that obtained results can be useful for enhancement of Mn acceptor concentration in $MgTiO_3$-based ceramics, as well as Mn^{4+} PL in $MgTiO_3$ red phosphors.

2. Materials and methods

The Mn-doped magnesium titanate ceramics were synthesized via sintering of MgO (98.8 %) and TiO_2 (99.73 %, a mixture of rutile and anatase phases) powders taken in different molar ratios (1:1, 1.19:1, 1.5:1 and 2:1) with adding of an aqueous solution of $MnSO_4$. The latter was taken in quantity necessary to provide 0.1 mol.% Mn concentration. Each powder mixture was thoroughly grinded in a ceramic mortar for 1 h. The propylene glycol used as a binder and aqueous solution of $MnSO_4$ were added to powder mixture and mixed until a homogeneous thick paste formed. The rectangular pellets of average size about $10 \times 10 \times 5\ mm^3$ were formed from the paste, dried at 150 °C for 3 h and sintered in the air at 1200 °C for 3 h in a muffle furnace. Sintered ceramic pellets were slowly cooled to room temperature as the furnace was naturally cooled down. The dense ceramic pellets were milled to obtain powders for further investigations.

Structural analysis was performed by X-ray diffraction (XRD) method in the θ-2θ geometry using Philips X'Pert PRO MRD diffractometer with CuK_α radiation. The topology and elemental analysis of sintered ceramic samples were studied using High-resolution scanning electron microscope Tescan Mira 3 LMU and Oxford Instruments energy dispersive spectrometer Oxford Instruments X-Max 80, respectively. The PL spectra were detected using a spectrometer equipped with a photomultiplier tube and excited by a 405 nm and 532 nm continuous diode lasers (50 mW) as well as by a light of Xe lamp (150 W) passed through a monochromator. The PL spectra were recorded at room and liquid nitrogen temperatures. Emission decay study was carried out at room temperature with 480 nm excitation wavelength and a 4 ns pulse duration generated by a "Continuum Horizon" OPO pumped with a Surelite frequency tripled Nd:YAG laser. The energy per pulse was approximately 20 mJ at the wavelength used. The repetition frequency was 10 Hz with 4 ns pulses. After dispersion by a monochromator ORIEL 1/4 m the luminescent transient signals were measured with a Hamamatsu 3896 PMT, sent to a digital oscilloscope, and averaged out to improve the signal-to-noise ratio. The diffuse reflectance spectra were recorded with a SILVER-Nova-TEC-X2 spectrometer (StellarNet, USA). The optical absorption spectra were recalculated from the diffuse reflectance spectra using the Kubelka-Munk theory. Electron paramagnetic resonance (EPR) study was carried out using X-band EPR spectrometer Varian E12 (~ 9.5 GHz) equipped by paired cavity that allows recording EPR signals from a standard (Mn-doped MgO sample) and a ceramic sample separately by modulation switching. The EPR spectra were normalized with respect to the intensity of the signal of a standard, as well as on the mass of each sample studied.

3. Results

In Fig. 1, the XRD patterns of the samples synthesized under various ratios of MgO and TiO_2 are shown. The ceramics fabricated under 1:1 ratio contains a major rhombohedral $MgTiO_3$ (ICDD PDF 010−75-3957) and a minor orthorhombic $MgTi_2O_5$ (ICDD PDF 010−89-6943) crystalline phases. This composition is typical for $MgTiO_3$ produced by sintering of MgO and TiO_2 powders [13]. The $MgTi_2O_5$ phase is generally formed in a minor amount as a second phase when sintering MgO and TiO_2 in equimolar proportions [13,25]. However, the phase composition changes as the excess MgO is added to the charge. The XRD patterns of the samples obtained with 1.19:1, 1.5:1 and 2:1 ratios demonstrate the peaks of both $MgTiO_3$ crystal phase and cubic Mg_2TiO_4 phase (ICDD PDF 010−73-1723). No traces of MgO phase are found. The increase of excess MgO content results in the increase of Mg_2TiO_4 phase and the decrease of $MgTiO_3$ phase concentrations. The ratios of Mg_2TiO_4 and $MgTiO_3$ phases estimated by Reference Intensity Ratio (RIR) method for the samples produced under 1.19:1 and 1.5:1 M ratios agree with charge composition (MgO and TiO_2 amounts). In the ceramics synthesized under 2:1 M ratio, the Mg_2TiO_4 phase dominates. This is to be expected since such ratio corresponds to stoichiometric composition of Mg_2TiO_4.

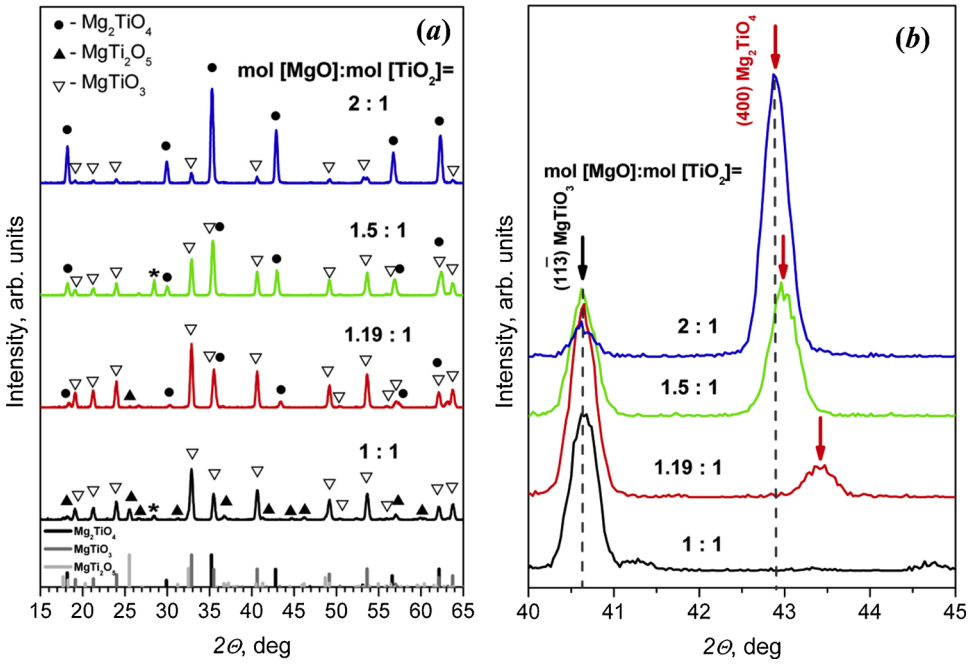

Fig. 1. XRD patterns of the powdered Mn-doped magnesium titanates sintered from MgO and TiO_2 of different molar ratios. The patters are shifted along y-axis for convenience. The PDF-cards of Mg_2TiO_4 and $MgTiO_3$ are shown by linear spectra. The peak at about 28° marked by the symbol * is due to Si wafer used as a holder.

However, the Mg_2TiO_4 is known to be unstable at temperatures lower than 1400 °C and suffers from decomposition into $MgTiO_3$ and MgO [26]. As a result, the secondary $MgTiO_3$ phase is usually observed when Mg_2TiO_4 is produced by solid state reaction in stoichiometric proportions of 2:1 [27,28]. Since the most intense XRD peaks of cubic MgO overlap with the XRD peaks of cubic Mg_2TiO_4, it is difficult to confirm the presence of MgO crystal phase as well as to estimate reliably the phase ratios in this ceramic sample.

The reactions of $MgTiO_3$ and $MgTi_2O_5$ phase formation can be described as follows:

$$MgO + TiO_2 \rightarrow MgTiO_3, \quad (1)$$

$$MgO + 2TiO_2 \rightarrow MgTi_2O_5, \quad (2)$$

It has been shown [5,25] that adding of excess MgO as low as 2 mol. % accelerates $MgTiO_3$ formation and inhibits formation of the $MgTi_2O_5$ in accordance with the reaction:

$$MgTi_2O_5 + MgO \rightarrow MgTiO_3. \quad (3)$$

However, excess MgO also promotes the appearance of Mg_2TiO_4 crystal phase [25]. The reactions of Mg_2TiO_4 formation and decomposition can be described as follows:

$$MgTiO_3 + MgO \rightarrow Mg_2TiO_4, \quad (4)$$

$$2MgO + TiO_2 \rightarrow Mg_2TiO_4, \quad (5)$$

$$Mg_2TiO_4 \rightarrow MgTiO_3 + MgO. \quad (6)$$

The adding of excess MgO to the charge does not affect the peak positions in XRD patterns for $MgTiO_3$ phase, while the peak positions of the Mg_2TiO_4 phase are found to be shifted towards larger angles 2θ as compared with the peak positions for unstrained Mg_2TiO_4 (Fig. 1b). The magnitude of the shift is the largest for the sample fabricated under 1.19:1 ratio. In particular, the shift of (400) diffraction peak of the Mg_2TiO_4 phase at 2θ = 42.8 degrees is about 0.5 degree (Fig. 1b). The shift magnitude decreases as the amount of excess MgO increases. The evaluated lattice parameter a of the cubic Mg_2TiO_4 phase was found to be less than the lattice parameter of unstrained Mg_2TiO_4 (a =8.4420 Å) and decreased from 8.4314 Å for 2:1 ratio, to 8.4089 Å for 1.5:1 ratio and to 8.3312 Å for 1.19:1 ratio. The Mg_2TiO_4 lattice shrinkage is apparently caused by the presence of excess point defects such as vacancies. Since the ceramics are sintered in the air and cooled slowly to room temperature, high concentration of oxygen vacancies is not expected. Therefore, these point defects are most likely the cation vacancies. This agrees with the fact that the lattice parameter depends on MgO to TiO_2 ratio, i.e. lattice shrinkage (compressive strains) decreases with the increase of excess MgO.

SEM images of cleaved ceramic's surfaces (Fig. 2, a–d) demonstrate similar dense structure with low porosity. The main ceramic body of all samples consists of well-sintered micron-sized grains. In the pores, the grains of different shapes are observed (Fig. 2, e–h). Some of them are faceted and contain the growth steps. The EDX analysis of the regions of about 10 × 10 μm^2 proved that Mg, Ti and O contents vary according to the MgO : TiO_2 molar ratio. In particular, the content of elements changes from [Mg] = 19 at%, [Ti] = 34 at%, [O] = 47 at% for 1:1 ratio to [Mg] = 20 at%, [Ti] = 26 at%, [O] = 54 at% for 1.19:1 ratio, and is [Mg] = 36 at%, [Ti] = 18 at%, [O] = 46 at% for 2:1 ratio. However, the EDX analysis of smaller micron-sized regions revealed noticeable variations in elemental composition over the certain ceramic body. In particular, in the ceramics of 1:1 and 1.19:1 ratios the regions with the reduced Mg content [Mg] = 7 at%, [Ti] = 53 at%, and [O] = 40 at% are found. In the ceramics of 1.19:1 ratio, the regions with the increased Mg and decreased Ti contents ([Mg] = 22 at%, [Ti] = 19 at%, [O] = 59 at%) are also observed. Such a large spread of composition reflects the presence of different magnesium titanate phases in the ceramic bodies.

As $MgTiO_3$ is produced via sintering of mixed MgO and TiO_2 powders, solid state chemical reaction between the components occurs during thermal treatment. The main transport mechanism is diffusion. Similarly to ZnO-Al_2O_3 pair, in MgO + TiO_2 powder mixture, diffusion of only one species into the other is considered, namely, faster diffusion of magnesium into titania grains is supposed [13,29]. The diffusion occurs in such a way that the product of reaction, $MgTiO_3$, forms as layers within an angle of certain aperture on the TiO_2 grains forming the neck growth regions between the MgO and TiO_2 grains [13]. Then, coalescence of neighbor grains takes place. This stage of sintering is captured in SEM images (Fig. 2). The faceted grains and the growth steps found on the grains in the pores (Fig. 2e–h) testify to vapor transport

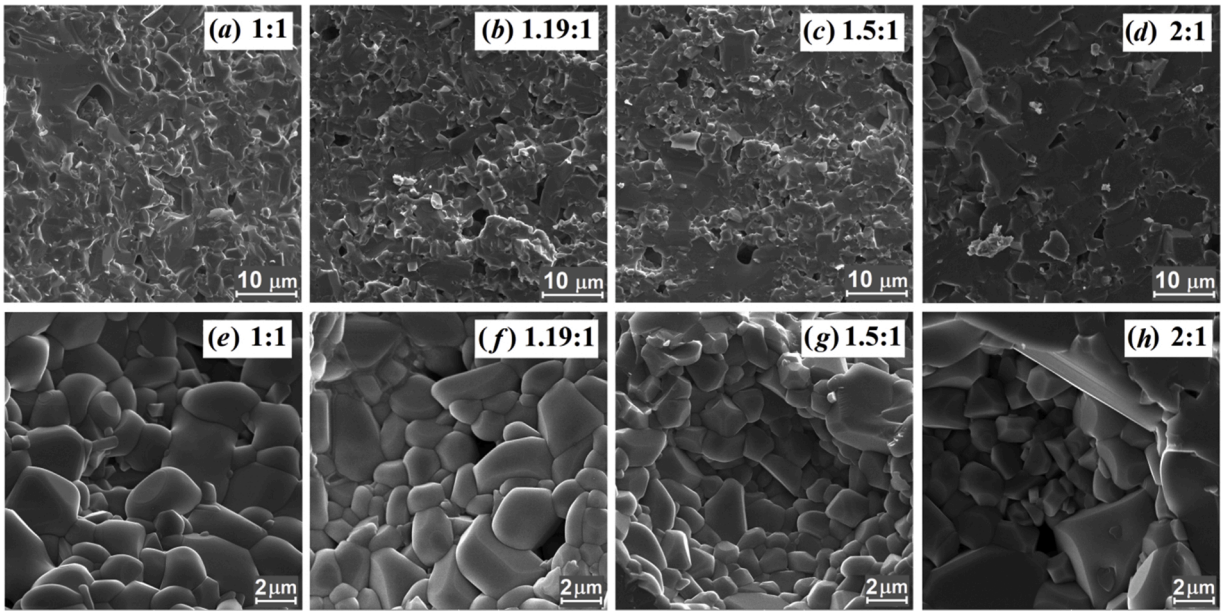

Fig. 2. SEM images of cleaved surface (a-d) and pore region (e-h) of Mn-doped magnesium titanate ceramics sintered from MgO and TiO_2 of different molar ratios.

accompanied by sublimation and condensation as one more transport mechanism contributing to sintering of ceramics studied.

In [29], analysis of magnesium titanate phases formed during sintering of MgO and rutile single crystals had shown that the reacted layer consisted mainly of thin Mg_2TiO_4 layer adjacent to MgO piece, thick $MgTiO_3$ layer and relatively thick $MgTi_2O_5$ layer adjacent to TiO_2.

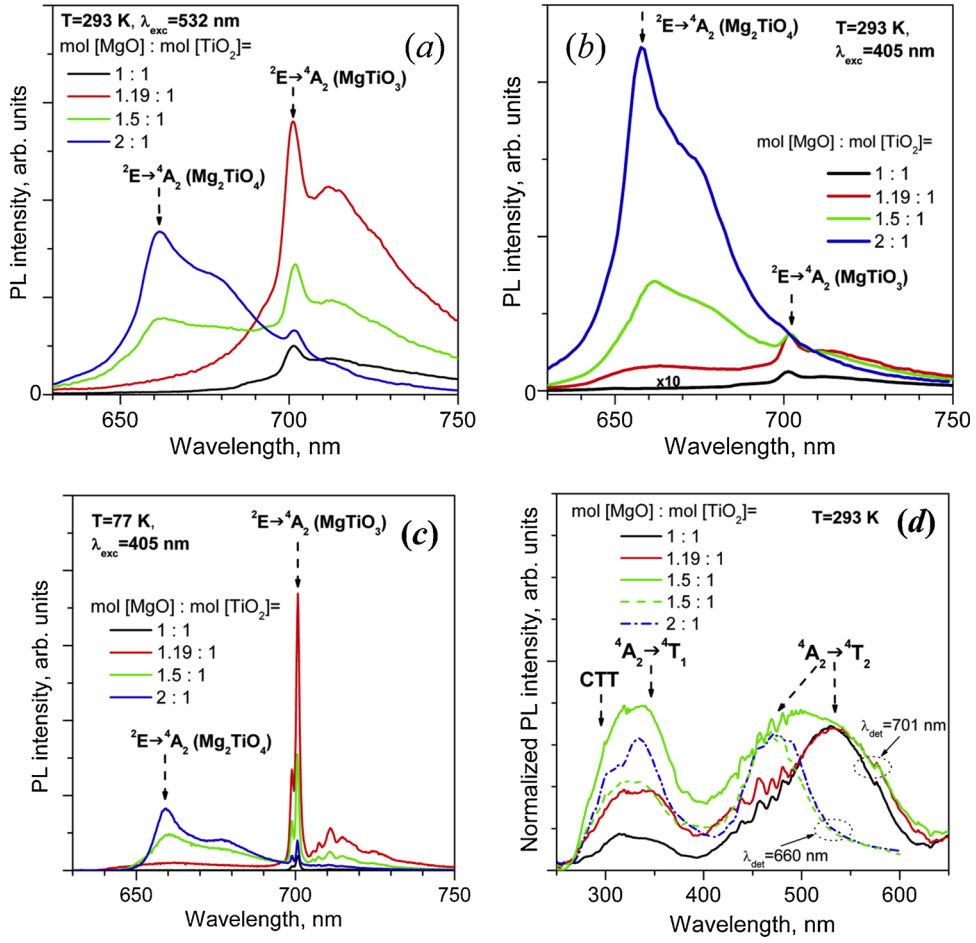

Fig. 3. PL (a, b, c) and normalized PL excitation spectra (d) of the Mn-doped ceramics sintered from MgO and TiO_2 of different molar ratios and detected at T =293 K (a, b, d) and 77 K (c) under 532 nm (a) and 405 nm (b, c) excitation lines and at 701 nm and 660 nm detection wavelengths (d).

Therefore, it is naturally to suppose that in the ceramics synthesized with 19 and 50 mol.% excess MgO formation of Mg_2TiO_4 and $MgTiO_3$ crystal phases occurs in the same order along the path of magnesium diffusion from MgO into TiO_2 grains. The one-way diffusion, which proceeds via vacancy mechanism is accompanied by opposite movement of the lattice vacancies, which gather in the material of faster diffusing species. Therefore, accumulation of Mg vacancies (V_{Mg}) can be expected in the Mg_2TiO_4 phase, and concentration of vacancies will be the higher, the smaller the Mg_2TiO_4 phase content. Thus, magnesium vacancies can be considered as the main reason of compressive strains in the Mg_2TiO_4 phase.

The room temperature PL spectra excited by 532 nm laser line (Fig. 3a) show red band with relatively narrow peak at 701 nm (R-line) caused by spin forbidden $^2E \rightarrow {}^4A_2$ transitions of Mn^{4+} ions in $MgTiO_3$. The lowest intensity of this PL is found in the ceramics synthesized under 1:1 M ratio. As 19 mol.% excess MgO is added, the emission increases by about 6 times. However, the increase of molar ratio to 1.5:1 and 2:1 produces gradual decrease of PL intensity.

The PL spectra recorded under 405 nm excitation show the similar tendencies, but with different variations of PL intensity (Fig. 3b). In particularly, adding of 19 mol.% excess MgO causes the increase of PL at 701 nm in 30 times with respect to the PL of the ceramics synthesized under 1:1 M ratio. At the same time, the PL intensity remains the same for 1.5:1 and 2:1 M ratio. This is apparently due to the contribution of the emission caused by Mn^{4+} ions in Mg_2TiO_4 phase, which arises starting from 19 mol.% excess MgO. The PL band due to Mn^{4+} in Mg_2TiO_4 is located in the red and is peaked at about 660 nm (R-line emission). It is more pronounced under UV excitation (Fig. 3b). The intensity of this emission increases as an amount of Mg_2TiO_4 phase increases according to the XRD data. In the ceramics synthesized with 19 mol.% excess MgO, the PL band is fully unstructured, and in the ceramics synthesized with 50 mol.% excess MgO the peak at about 660 nm becomes noticeable. It should be noted that as the excess MgO content increases, the PL peak position slightly shifts towards shorter wavelengths (on about 2 nm), and a relative intensity of R-line decreases as well as the band broadens at least in the short wavelength region.

It can be supposed that low intensity of R-line is related to the presence of V_{Mg} and corresponding deformations of oxygen octahedron in which Mn^{4+} is incorporated. It has been proposed [30] that if the Mn^{4+} ion is located in non-centrosymmetric site (absence of inversion symmetry), the parity selection rule for $^2E \rightarrow {}^4A_2$ transition relaxes, the electric dipole intensity increases and the R-line intensity increases. Therefore, it can be supposed that compressive stress results in more centrosymmetric site for octahedral coordinated Mn^{4+} ion in Mg_2TiO_4. Deformation of oxygen octahedron can also affect splitting of Mn^{4+} emitting levels, and nonuniform stresses can cause lost of the structure of the emission band.

The low temperature PL spectra of the ceramics excited by 405 nm laser line show the same trends for Mn^{4+} emission spectra via excess MgO content as the room temperature spectra (Fig. 3c). The difference is that the intensity of Mn^{4+} PL in the $MgTiO_3$ phase increases stronger than in the Mg_2TiO_4 phase upon cooling to liquid nitrogen temperature. This is apparently due to more intense thermal quenching of Mn^{4+} PL in $MgTiO_3$ as compared with Mg_2TiO_4 [8,31].

The excitation spectra of Mn^{4+} PL in $MgTiO_3$ detected at 701 nm show two broad bands centered at 325 and 535 nm (Fig. 3d). The UV band is due to both charge transfer transition (CTT) and $^4A_2 \rightarrow {}^4T_1$ transition, and the green band corresponds to $^4A_2 \rightarrow {}^4T_2$ spin allowed transition of Mn^{4+} ions in $MgTiO_3$. In the ceramics obtained under equimolar ratio of MgO and TiO_2, the intensity of green excitation band significantly exceeds the intensity of the UV band. When the excess MgO is added, relative intensity of the UV excitation band becomes higher. In addition, the green excitation band expands to the blue. The broadening of the excitation band is apparently caused by contribution of Mn^{4+} PL of the Mg_2TiO_4 phase. In fact, in the ceramics produced under 1.19:1 and 2:1 ratio, the PL excitation spectra detected at 660 nm (Fig. 3d) are found to be similar.

Fig. 4a shows the PL decay curves in the ceramics studied. In the sample produced under 1:1 ratio, the decay curve of 701 nm emission shows a single exponential behavior with a PL decay time of 17 μs. The relaxation of PL at 660 nm occurs with decay time of 14 μs (Fig. 4b). These magnitudes agree well with decay time of 25 μs reported for Mn^{4+} emission in the $MgTiO_3$ [8] and can be explained by intense PL thermal quenching at room temperature. At the same time, the PL decay curves of the ceramics with 19 and 50 mol.% excess MgO contain the regions of faster and slower decline. The PL decay times of slower decline region are in the range of 0.40−0.45 ms (Table 1). In these samples, the relaxation of the PL at 660 nm occurs with similar decay times of 0.44−0.50 ms (Table 1). These values are close to PL decay times reported for Mn^{4+} PL in Mg_2TiO_4 [23]. Therefore, the region of slower decline is apparently caused by contribution of Mn^{4+} emission in the Mg_2TiO_4 phase [10]. The decay time of this PL is the smallest in the sample with the largest compressive strains in the Mg_2TiO_4 grains (1.19:1 ratio). This implies that deformations in Mg_2TiO_4 affect not only the shape of Mn^{4+} PL spectrum, but also the PL decay. At room temperature the relaxation times of Mn^{4+} PL in Mg_2TiO_4 and $MgTiO_3$ are influenced by contribution of non radiative recombination caused by PL thermal quenching [8,12]. The latter is usually ascribed to thermally activated crossing of the Mn^{4+} $^4A_2$ ground state and some excited state ($^4T_2$ state or CTT). Thus, the shortening of PL relaxation time is probably due to the increased contribution of PL thermal quenching. In the samples with excess MgO, a noticeable slowing down of PL relaxation is found for the region of faster decline (Fig. 4b). However, because of changing slope it is difficult to say whether the decay time of Mn^{4+} PL in the $MgTiO_3$ increases or not with adding of excess MgO.

The optical absorption of the ceramics also changes with adding of excess MgO. The sample produced with stoichiometric ratio 1:1 has no pronounced color, and those with 19 mol.% excess MgO is pink. As the excess MgO content increases, the color acquires a brownish yellow tint, apparently due to contribution of optical absorption in Mn^{4+} activated Mg_2TiO_4 phase. In fact, the absorption spectrum of the ceramics with 19 mol.% excess MgO (Fig. 5) indicates that a pink color is due to absorption band peaked at about 540 nm and stretched to the red. This band is apparently caused by $^4A_2 \rightarrow {}^4T_2$ transition of Mn^{4+} ions in the $MgTiO_3$ phase. The same band of smaller intensity in found in the absorption spectrum of the ceramics produced with 1:1 ratio. The rise of this absorption with adding of excess MgO indicates the increase of concentration of Mn^{4+} centers in the $MgTiO_3$ host. In the ceramics with 50 mol.% excess MgO, intensity of this band decreases and another one at about 480 nm arises. This absorption band is obviously due to $^4A_2 \rightarrow {}^4T_2$ transition of Mn^{4+} ions in the Mg_2TiO_4 phase and its intensity agrees with content of Mg_2TiO_4 phase in the ceramics.

The EPR spectra of the Mn-doped ceramics presented in Fig. 6 show the same sextets of lines with the g-factor about 2.00. This signal is apparently originated from Mn ions in $MgTiO_3$ phase. The experimental spectra were simulated using the program Powder included in the software package Visual-EPR [32]. The program is based on an algorithm that uses an exact solution of the spin-Hamiltonian including electron Zeeman interaction, the fine and hyperfine interactions. The spin-Hamiltonian parameters of the simulated signal are derived as follows: g-factor value is 2.004, fine-structure parameter $b_2 = 0.0165$ cm^{-1} and ultrafine-structure parameter $A = 0.0079$ cm^{-1}. These magnitudes agree well with the parameters of Mn^{2+} ions ($S = 5/2$) in crystal lattice of $MgTiO_3$ reported by other authors [33,34]. The adding of excess MgO promotes the decrease of both the intensity and halfwidth of the EPR signal (Fig. 6) that indicates the decrease of concentration of the Mn^{2+} centers. The concentration of Mn^{2+} ions in $MgTiO_3$ phase was evaluated taking into account the weight content of this phase in the ceramics estimated by RIR method from the XRD patterns. The concentration decreases from $9 \cdot 10^{19}$ spin g^{-1} for 1:1 ratio (72 wt.% of $MgTiO_3$) to $1.7 \cdot 10^{19}$ spin g^{-1} for 1.19:1 ratio (77 wt.% of $MgTiO_3$) and to $4.5 \cdot 10^{18}$ spin g^{-1} for 1.5:1 ratio (44 wt.% of $MgTiO_3$).

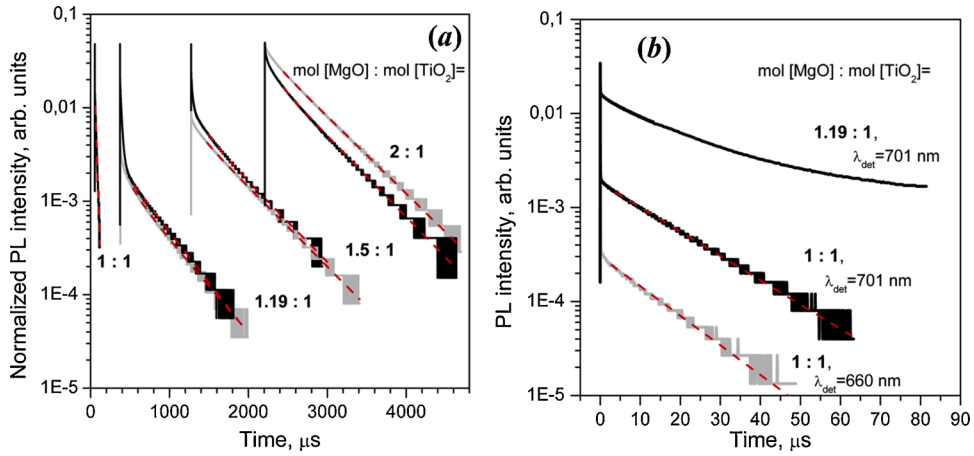

Fig. 4. PL decay curves detected at 701 nm (black) and 660 nm (gray) for the ceramics produced from MgO and TiO_2 of different molar ratios and their approximation by exponential dependence (dotted lines). The curves on (a) are shifted on time axis for convenience.

Table 1
PL decay times obtained from approximation by exponential dependence of PL relaxation detected at 701 and 660 nm for the ceramics produced from MgO and TiO_2 of different molar ratios.

MgO to TiO_2 molar ratio, mol [MgO] : mol [TiO_2]	PL decay time, μs (detected at 701 nm)	PL decay time, μs (detected at 660 nm)
1 : 1	17	14
1.19 : 1	405	438
1.5 : 1	453	500
2 : 1	499	520

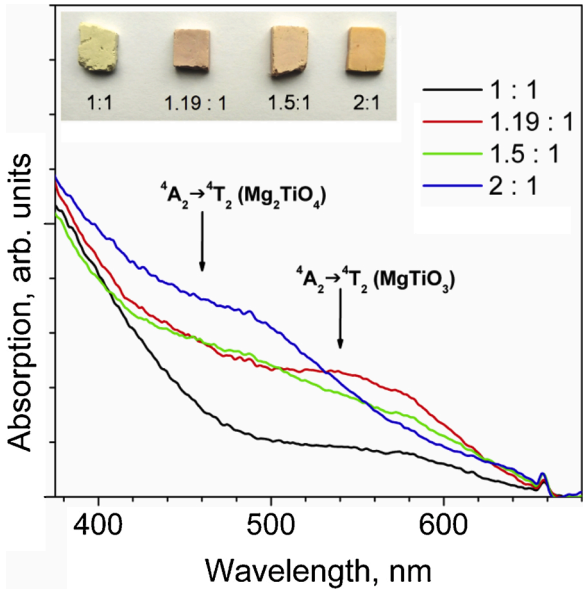

Fig. 5. Room temperature optical absorption spectra of the Mn-doped ceramics sintered from MgO and TiO_2 of different molar ratios.

It should be noted that no EPR sextets caused by Mn^{4+} ion in $MgTiO_3$ were detected even in the ceramics with excess MgO content that showed the pronounced Mn^{4+} absorption and PL. In fact, the Mn^{4+} ion (S = 3/2) is usually characterized by lower value of g-factor and much higher fine constant than the Mn^{2+} ion [35]. Due to the latter, the signal from Mn^{4+} ions can also be observed in the low field region. This is often used as a signature of Mn^{4+} [35,36]. No signal that can be ascribed to

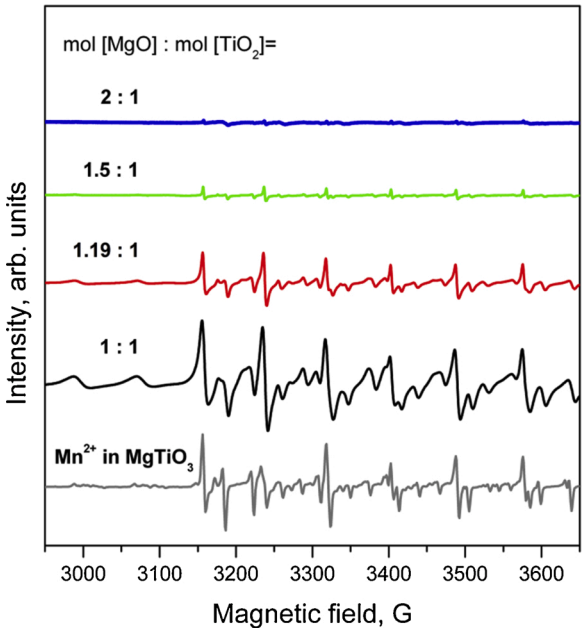

Fig. 6. Experimental EPR spectra of Mn-doped ceramics sintered from MgO and TiO_2 of different molar ratios and simulated spectrum of Mn^{2+} ion in $MgTiO_3$.

Mn^{4+} ions was observed in this region. The possible reason can be the adverse relaxation conditions for Mn^{4+} ions, i. e. too short or too long spin relaxation times.

4. Discussion

$MgTiO_3$ has the trigonal "ilmenite'' structure, which consists of a close-packed-hexagonal O^{2-} anion sublattice that has 2/3 of its octahedral sites occupied alternately by Mg^{2+} and Ti^{4+} cations [37]. When Mn incorporates into crystal lattice of $MgTiO_3$, it can replace the sites of the host Mg^{2+} as Mn^{2+} and Ti^{4+} as Mn^{4+} without the need for charge compensation. Taking into account similarity of the ionic radii of corresponding Mn ions and the host cations (r(Mn^{4+}, VI) = 0.53 Å, r(Ti^{4+}, VI) = 0.605 Å, r(Mn^{2+}, VI) = 0.67 Å (low spin), r (Mg^{2+}, VI) = 0.72 Å), it is difficult to conclude which cation (Ti^{4+} or Mg^{2+}) manganese prefers to substitute. The EPR spectra of the ceramics sintered in stoichiometric molar ratio of 1:1 reveal the Mn^{2+} ions in concentration close to nominal concentration of Mn dopant. This means that manganese tends to

incorporate into $MgTiO_3$ as Mn^{2+} on Mg site. This can be an important reason of low intensity of Mn^{4+} PL. It should be noted, that Mn^{2+} ions might also enter the Ti^{4+} sites being compensated by oxygen vacancy defects. Such situation has been observed in Mn-doped $BaTiO_3$ ceramics sintered in oxygen deficient atmosphere [38,39]. It has been shown that Mn on Ti site in $BaTiO_3$ gradually changes its valence from +4 to +3 and finally to +2 with decreasing oxygen partial pressure from 1 atm at elevated temperatures [39]. However, considering sintering conditions of the ceramics studied (the ambient atmosphere and slow cooling to room temperature), the observed intense EPR signal should be ascribed to Mn^{2+} ions on Mg^{2+} site.

It should be noted that optical absorption data do not show specific features caused by optical transitions of Mn^{2+} ions in the $MgTiO_3$. Usually, absorption spectrum of Mn^{2+} ions in tetrahedral and octahedral sites composes of several narrow and wider bands lying in the UV and blue-green spectral ranges. However, all transitions from the ground to the excited levels of Mn^{2+} are spin-forbidden contrary to spin allowed $^4A_2 \rightarrow {}^4T_1$ and $^4A_2 \rightarrow {}^4T_2$ transitions of Mn^{4+} found in the same spectral regions. Therefore, even if the concentrations of Mn^{2+} and Mn^{4+} centers are comparable, optical absorption due to Mn^{2+} ions can be hidden by Mn^{4+} transitions. In $MgTiO_3$, the Mn^{2+} ions occupy the octahedrally coordinated lattice sites and can show a structureless PL band in the orange-red spectral region. However, because of weak excitation the Mn^{2+} PL will be of low intensity and hardly distinguishable on the background of Mn^{4+} red PL.

The results of the EPR and optical studies show that adding of excess MgO promotes the decrease of concentration of Mn^{2+} ions and the increase of Mn^{4+} ion concentration in the $MgTiO_3$ phase. It is naturally to suppose that excess MgO hinders substitution for Mg site ions with Mn^{2+} and promotes incorporation of Mn^{4+} onto Ti^{4+} site. This is similar to a long time ago discovered Ca acceptor behavior in $BaTiO_3$ ceramics sintered under BaO excess [40]. It has been shown that when there is an excess of alkaline earth oxide ((Ca + Ba)/Ti>1), some Ca^{2+} ions, which are well known Ba site substituents in $BaTiO_3$, occupy Ti sites where they act as doubly charged acceptors and compensate oxygen vacancies acting as shallow donors. The Ca acceptor behavior was proved by the electrical conductivity measurements [41] and Atom Location Using Channeling-Enhanced Microanalysis measurements [40]. Similarly, in Mn-doped Mg_2TiO_4 phosphor, the enhancement of manganese incorporation onto the Ti site with adding of excess MgO has been found [23].

The results of EPR study show that concentration of Mn^{2+} in $MgTiO_3$ phase gradually decreases as the excess MgO increases, which suggest gradual increase of Mn^{4+} concentration. However, the intensity of PL at 701 nm shows non-monotonic dependence on excess MgO content (Fig.2a). The largest intensity of Mn^{4+} PL is found for 19 mol.% excess MgO. The decrease of PL intensity for 1.5:1 and 2:1 M ratio can be ascribed to the decrease of amount of $MgTiO_3$ phase in the ceramics (44 and 17 wt.%, respectively, as opposed to 77 wt.% for the ceramics synthesized with 1.19:1 ratio).

Therefore, the rise of Mn^{4+} concentration can be considered as the main reason of the PL intensity increase in $MgTiO_3$ ceramics with excess MgO. The increase is larger for UV excitation than for 532 nm excitation. The difference can be explained by the decrease of the excitation light absorption by the $MgTi_2O_5$ secondary phase. In fact, the $MgTi_2O_5$ shows smaller band gap of 3.9 eV [42] as compared with 4.2 eV of $MgTiO_3$ [43,44] and 4.33 eV of Mg_2TiO_4 [23,45]. Therefore, direct band-to-band transitions in $MgTi_2O_5$ can cause strong absorption of UV excitation light in the ceramics produced under 1:1 ratio.

The obtained results show that excess MgO not only affects crystal phase formation, but also changes the manner of Mn incorporation in crystal lattice of $MgTiO_3$. This should be taken into account when using Mn-doped $MgTiO_3$ as a component of dielectric ceramics or as a red phosphor. In particular, the adding of excess MgO can be considered as an efficient tool for the increasing of Mn acceptor concentration as well as Mn^{4+} PL intensity in $MgTiO_3$.

5. Conclusions

The effect of excess MgO on Mn^{4+} emission and crystal phase formation in Mn-doped magnesium titanates produced by a solid state reaction has been investigated. The samples synthesized using equimolar ratio of MgO and TiO_2 contained the major $MgTiO_3$ phase and minor $MgTi_2O_5$ phase. The EPR study revealed intense EPR signal due to Mn^{2+} in $MgTiO_3$, the estimated concentration of Mn^{2+} centers is found to be close to nominal content of Mn dopant. It is concluded that in addition to PL thermal quenching, both preferential incorporation of Mn onto Mg^{2+} site and formation of secondary $MgTi_2O_5$ phase, that causes strong absorption of the UV excitation light, are responsible for low intensity of Mn^{4+} PL in $MgTiO_3$. The ceramics synthesized with excess MgO were composed of the $MgTiO_3$ and Mg_2TiO_4 crystal phases in different weight proportions and demonstrated red PL due to Mn^{4+} ions onto Ti^{4+} site in these phases. The Mg_2TiO_4 phase is found to be under compressive strains originated from intrinsic defects (presumably, magnesium vacancies). The lattice parameter of Mg_2TiO_4 crystal phase as well as spectral shape and decay times of red PL due to Mn^{4+} in the Mg_2TiO_4 are shown to be strongly affected by MgO to TiO_2 ratio. In the $MgTiO_3$ phase, the adding of excess MgO produces successive decrease of Mn^{2+} ion concentration and the increase of Mn^{4+} PL intensity. The increase of Mn^{4+} optical absorption testified the increased concentration of Mn^{4+} centers. It is supposed that excess MgO hinders substitution for Mg site by Mn^{2+} ions and promotes the incorporation of Mn^{4+} ion onto Ti^{4+} site in $MgTiO_3$. The adding of excess MgO can be considered as an efficient tool for the increase of Mn^{4+} PL intensity in $MgTiO_3$.

CRediT authorship contribution statement

L. Borkovska: Conceptualization, Writing - original draft, Supervision. **L. Khomenkova:** Investigation, Formal analysis, Writing - review & editing. **T. Stara:** Investigation, Formal analysis. **I. Vorona:** Investigation, Conceptualization, Writing - original draft. **V. Nosenko:** Investigation, Formal analysis. **O. Gudymenko:** Investigation, Formal analysis. **V. Kladko:** Conceptualization, Writing - review & editing. **K. Kozoriz:** Investigation. **C. Labbé:** Investigation, Writing - review & editing, Supervision. **J. Cardin:** Writing - review & editing. **J.-L. Doualan:** Investigation. **T. Kryshtab:** Conceptualization, Writing - original draft.

Declaration of Competing Interest

The authors declare that they have no known competing financial interests or personal relationships that could have appeared to influence the work reported in this paper.

Acknowledgements

This work was partly supported by National Academy of Sciences of Ukraine (project III-10-18) as well as via the bilateral program DNIPRO (project M/34-2020 in Ukraine and #42549TM in France) funded by the Ministry of Education and Research of Ukraine, by the Ministries of Foreign Affairs and International Development (MAEDI) and the Ministry of Education, Higher Education and of Research (MENESR) in France. The authors thank Prof. Melnichuk O.V. from Mykola Gogol Nizhyn State University (Nizhyn, Ukraine) for the help with measurements of diffuse reflectance spectra.

References

[1] C. Chen, Z. Peng, L. Xie, K. Bi, X. Fu, Microwave dielectric properties of novel $(1-x)MgTiO_3$–$xCa_{0.5}Sr_{0.5}TiO_3$ ceramics, J. Mater. Sci.: Mater. Electron. 31 (2020) 13696–13703, https://doi.org/10.1007/s10854-020-03927-1.

[2] K. Wakino, Recent development of dielectric resonator materials and filters in Japan, Ferroelectrics. 91 (1989) 69–86, https://doi.org/10.1080/00150198908015730.

[3] V.M. Ferreira, J.L. Baptista, S. Kamba, J. Petzelt, Dielectric spectroscopy of $MgTiO_3$-based ceramics in the 10^9–10^{14} Hz region, J. Mater. Sci. 28 (1993) 5894–5900, https://doi.org/10.1007/BF00365198.

[4] M. Zhang, L. Li, W. Xia, Q. Liao, Structure and properties analysis for $MgTiO_3$ and $(Mg_{0.97}M_{0.03})TiO_3$ (M = Ni, Zn, Co and Mn) microwave dielectric materials, J. Alloys. Compd. 537 (2012) 76–79, https://doi.org/10.1016/j.jallcom.2012.05.026.

[5] Z. Xu, L. Li, S. Yu, M. Du, W. Luo, Magnesium fluoride doped $MgTiO_3$ ceramics with ultra-high Q value at microwave frequencies, J. Alloys. Compd. 802 (2019) 1–5, https://doi.org/10.1016/j.jallcom.2019.06.207.

[6] C. Vigreux, B. Deneuve, J. El Fallah, J.M. Haussonne, Effects of acceptor and donor additives on the properties of $MgTiO_3$ ceramics sintered under reducing atmosphere, J. Eur. Ceram. Soc. 21 (2001) 1681–1684, https://doi.org/10.1016/S0955-2219(01)00092-9.

[7] V. Dordevic, M.G. Brik, A.M. Srivastava, M. Medic, P. Vulic, E. Glais, B. Viana, M. D. Dramicanin, Luminescence of Mn^{4+} ions in $CaTiO_3$ and $MgTiO_3$ perovskites: relationship of experimental spectroscopic data and crystal field calculations, Opt. Mater. 74 (2017) 46–51, https://doi.org/10.1016/j.optmat.2017.03.021.

[8] E. Glais, V. Dordevic, J. Papan, B. Viarna, M.D. Dramicanin, $MgTiO_3$:Mn^{4+} a multi-reading temperature nanoprobe, RSC Adv. 8 (2018) 18341–18346, https://doi.org/10.1039/C8RA02482K.

[9] L. Lv, S. Wang, X. Wang, L. Han, Inducing luminescent properties of Mn^{4+} in magnesium titanate systems: an experimental and theoretical approach, J. Alloys. Compd. 750 (2018) 543–553, https://doi.org/10.1016/j.jallcom.2018.03.322.

[10] J. Long, C. Ma, Y. Wang, X. Yuan, M. Du, R. Ma, Z. Wen, J. Zhang, Y. Cao, Luminescent performances of Mn^{4+} ions during the phase evolution from $MgTiO_3$ to Mg_2TiO_4, Mater. Res. Bull. 85 (2017) 234–239, https://doi.org/10.1016/j.materresbull.2016.09.015.

[11] Z. Zhou, N. Zhou, M. Xia, Y. Meiso, H.T. (Bert) Hintzen, Research progress and application prospect of transition metal Mn^{4+}-activated luminescent materials, J. Mater. Chem. C 4 (2016) 9143–9161, https://doi.org/10.1039/C6TC02496C.

[12] R. Louat, A. Louat, E. Duval, Temperature dependence of the Mn^{4+} R-Lines and vibronic transitions in $MgTiO_3$ and Mg_2TiO_4, Phys. Status Solidi B 46 (1971) 559–565, https://doi.org/10.1002/pssb.2220460212.

[13] F. Cambier, C. Leblud, M.R. Anseau, Reaction sintering of MgO-TiO_2 mixtures, Ceram. Int. 8 (1982) 77–78, https://doi.org/10.1016/0272-8842(82)90020-7.

[14] G. Villela, Y. Saikali, A. Louat, J. Paris, F. Gaume-Mahn, Le metatitanate de magnesium, nouvelle matrice pour l'etude de la fluorescence de l'ion Mn^{4+}. Preparation et proprietes de luminescence, J. Phys. Chem. Solids 30 (1969) 2599–2605, https://doi.org/10.1016/0022-3697(69)90268-6.

[15] J. Lu, Y. Pan, J. Wang, X. Chen, S. Huang, G. Liu, Reduction of Mn^{4+} to Mn^{2+} in $CaAl_{12}O_{19}$ by co-doping charge compensators to obtain tunable photoluminescence, RSC Adv. 3 (2013) 4510–4513, https://doi.org/10.1039/C3RA22938F.

[16] T. Senden, R.J.A. van Dijk-Moes, A. Meijerink, Quenching of the red Mn^{4+} luminescence in Mn^{4+}-doped fluoride LED phosphors, Light Sci. Appl. 7 (2018), https://doi.org/10.1038/s41377-018-0013-1, 8.

[17] F. Garcia-Santamaria, J.E. Murphy, A.A. Setlur, S.P. Sista, Concentration quenching in K_2SiF_6:Mn^{4+} phosphor, ECS J. Solid State Sci. Technol. 7 (2018) 3030–3033. https://iopscience.iop.org/article/10.1149/2.0081801jss.

[18] R. Cao, J. Huang, X. Ceng, Z. Luo, W. Ruan, Q. Hu, $LiGaTiO_4$:Mn^{4+} red phosphor: synthesis, luminescence properties and emission enhancement by Mg^{2+} and Al^{3+} ions, Ceram. Int. 42 (2016) 13296–13300, https://doi.org/10.1016/j.ceramint.2016.05.138.

[19] M. Peng, X. Yin, P.A. Tanner, M.G. Brik, P. Li, Site occupancy preference, enhancement mechanism, and thermal resistance of Mn^{4+} red luminescence in $Sr_4Al_{14}O_{25}$: Mn^{4+} for warm WLEDs, Chem. Mater. 27 (2015) 2938–2945, https://doi.org/10.1021/acs.chemmater.5b00226.

[20] D. Chen, Y. Zhou, W. Xu, J. Zhong, Z. Ji, W. Xiang, Enhanced luminescence of Mn^{4+}:$Y_3Al_5O_{12}$ red phosphor via impurity doping, J. Mater. Chem. C 4 (2016) 1704–1712, https://doi.org/10.1039/C5TC04133C.

[21] T. Murata, T. Tanoue, M. Iwasaki, K. Morinaga, T. Hase, Fluorescence properties of Mn^{4+} in $CaAl_{12}O_{19}$ compounds as red-emitting phosphor for white LED, J. Lumin. 114 (2005) 207–212, https://doi.org/10.1016/j.jlumin.2005.01.003.

[22] Y.X. Pan, G.K. Liu, Influence of Mg^{2+} on luminescence efficiency and charge compensating mechanism in phosphor $CaAl_{12}O_{19}$:Mn^{4+}, J. Lumin. 131 (2011) 465–468, https://doi.org/10.1016/j.jlumin.2010.11.014.

[23] L. Borkovska, L. Khomenkova, I. Vorona, V. Nosenko, T. Stara, O. Gudymenko, V. Kladko, C. Labbé, J. Cardin, A. Kryvko, T. Kryshtab, The role of excess MgO in the intensity increase of red emission of Mn^{4+}-activated Mg_2TiO_4 phosphors, J. Mater. Sci.: Mater. Electron. 31 (2020) 7555–7564, https://doi.org/10.1007/s10854-020-03143-x.

[24] C.-F. Shih, W.-M. Li, K.-S. Tung, C.-Y. Hsiao, K.-T. Hung, Microwave dielectric properties of $MgTiO_3$ by sintering MgO and TiO_2 nanostructures, in: Extended Abstracts of the 2009 International Conference on Solid State Devices and Materials, Sendai, 2009, pp. 563–564, https://doi.org/10.7567/SSDM.2009.P-8-6.

[25] K. Sreedhar, N.R. Pavaskar, Synthesis of $MgTiO_3$ and $Mg_4Nb_2O_9$ using stoichiometrically excess MgO, Mater. Lett. 53 (2002) 452–455, https://doi.org/10.1016/S0167-577X(01)00525-0.

[26] B.A. Wechsler, A. Navrotsky, Thermodynamics and structural chemistry of compounds in the system MgO-TiO_2, J. Solid State Chem. 55 (1984) 165–180, https://doi.org/10.1016/0022-4596(84)90262-7.

[27] A. Belous, O. Ovchar, D. Durilin, M.M. Krzmanc, M. Valant, D. Suvorov, High-q microwave dielectric materials based on the spinel Mg_2TiO_4, J. Am. Ceram. Soc. 89 (2006) 3441–3445, https://doi.org/10.1111/j.1551-2916.2006.01271.x.

[28] M.R.S. Silva, S.C. Souza, I.M.G. Santos, M.R. Cassia-Santos, L.E.B. Soledade, A. G. Souza, S.J.G. Lima, E. Longo, Stability studies on undoped and doped Mg_2TiO_4, obtained by the polymeric precursor method, J. Therm. Anal. Calorim. 79 (2005) 421–424, https://doi.org/10.1007/s10973-005-0077-z.

[29] G. Yamaguchi, T. Tokuda, Some aspects of solid state reactions between oxides, Bull. Chem. Soc. Jpn. 40 (1967) 843–851, https://doi.org/10.1246/bcsj.40.843.

[30] M.G. Brik, W.W. Beers, W. Cohen, S.A. Payne, N.J. Cherepy, M. Piasecki, A. M. Srivastava, On the Mn^{4+} R-line emission intensity and its tunability in solids, Opt. Mater. (Amst) 91 (2019) 338–343, https://doi.org/10.1016/j.optmat.2019.03.046.

[31] F.A. Kroger, W. Hoogenstraaten, M. Bottema, Th.P.J. Botden, The influence of temperature quenching on the decay of fluorescence, Physica 14 (1948) 81–96, https://doi.org/10.1016/0031-8914(48)90028-7.

[32] http://www.visual-epr.com.

[33] E.L. Carranza, R.T. Cox, ESR study of Fe^{3+} and Mn^{2+} ions on trigonal sites in ilmenite structure $MgTiO_3$, J. Phys. Chem. Solids 40 (1979) 413–420, https://doi.org/10.1016/0022-3697(79)90055-6.

[34] A.F.M.Y. Haider, A. Edgar, ESR study of transition metal ions in magnesium titanate, J. Phys. C: Solid State Phys. 13 (1980) 6239–6250, https://doi.org/10.1088/0022-3719/13/33/022.

[35] R.R. Rakhimov, A.L. Wilkerson, G.B. Loutts, M.A. Noginov, N. Noginova, W. Lindsay, H.R. Ries, Spin and valence states of manganese ions in manganese-doped yttrium orthoaluminate, Solid State Commun. 108 (1998) 549–554, https://doi.org/10.1016/S0038-1098(98)00403-7.

[36] T. Ye, S. Li, X. Wu, M. Xu, X. Wei, K. Wang, H. Bao, J. Wang, J. Chen, Sol-gel preparation of efficient red phosphor Mg_2TiO_4:Mn^{4+} and XAFS investigation on the substitution of Mn^{4+} for Ti^{4+}, J. Mater. Chem. 1 (2013) 4327–4333, https://doi.org/10.1039/C3TC30553H.

[37] G. Shirane, D.E. Cox, W.J. Takei, S.L. Ruby, A study of the magnetic properties of the $FeTiO_3$-αFe_2O_3 system by neutron diffraction and the mössbauer effect, J. Phys. Soc. Jpn. 17 (1962) 1598–1611, https://doi.org/10.1143/JPSJ.17.1598.

[38] H.-J. Hagemann, D. Hennings, Reversible weight change of acceptor-doped $BaTiO_3$, J. Am. Ceram. Soc. 64 (1981) 590–594, https://doi.org/10.1111/j.1151-2916.1981.tb10223.x.

[39] D.-K. Lee, H.-I. Yoo, K.D. Becker, Nonstoichiometry and defect structure of Mn-doped BaTiO3−δ, Solid State Ion. 154–155 (2002) 189–193, https://doi.org/10.1016/S0167-2738(02)00427-7.

[40] H.M. Chan, M.P. Harmer, M. Lal, D.M. Smyth, Calcium site occupancy in $BaTiO_3$, Mater. Res. Soc. Symp. Proc. 31 (1983) 345–350, https://doi.org/10.1557/PROC-31-345.

[41] D.F.K. Hennings, H. Schreinemacher, Ca-acceptors in dielectric ceramics sintered in reducive atmospheres, J. Eur. Ceram. Soc. 15 (1995) 795–800, https://doi.org/10.1016/0955-2219(95)00043-T.

[42] M.A. Ehsan, R. Naeem, V. McKee, A.S. Hakeem, M. Mazhar, $MgTi_2O_5$ thin films from single molecular precursor for photoelectrochemical water splitting, Sol. Energy Mater. Sol. Cells 161 (2017) 328–337, https://doi.org/10.1016/j.solmat.2016.12.015.

[43] T.S. Kumar, R.K. Bhuyan, D. Pamu, Effect of post annealing on structural, optical and dielectric properties of $MgTiO_3$ thin films deposited by RF magnetron sputtering, Appl. Surf. Sci. 264 (2013) 184–190, https://doi.org/10.1016/j.apsusc.2012.09.168.

[44] L.V. Borkovska, L. Khomenkova, I.V. Markevich, M. Osipyonok, T. Stara, O. Gudymenko, V. Kladko, M. Baran, S. Lavoryk, X. Portier, T. Kryshtab, Effect of Li^+ co-doping on structural and luminescence properties of Mn^{4+} activated magnesium titanate films, J. Mater. Sci.: Mater. Electron. 29 (2018) 15613–15620, https://doi.org/10.1007/s10854-018-9153-6.

[45] R.K. Bhuyan, T.S. Kumar, A. Perumal, S. Ravi, D. Pamu, Optical properties of ambient temperature grown nanocrystalline Mg_2TiO_4 thin films, Surf. Coat. Technol. 221 (2013) 196–200, https://doi.org/10.1016/j.surfcoat.2013.01.048.